Nanofiber Alignment on a Flexible Substrate: Hierarchical Order from Macro to Nano

Yogesh Ner,[†] Chris Asemota,[†] James R. Olson,[‡] and Gregory A. Sotzing*,[†,§]

The Polymer Program, Institute of Materials Science, and Department of Chemistry, University of Connecticut, 97 N. Eagleville Road, Storrs, Connecticut 06269, and Teleflex Medical, 1295 Main Street, P.O. Box 219, Coventry, Connecticut 06238

ABSTRACT A simplified approach to constructing a composite material comprised of aligned electrospun nanofibers onto a flexible substrate consisting of a microfilament yarn is presented. The metal-coated knit patterns of the microfilament yarn play the role of the parallel electrode, required for the alignment of electrospun nanofibers. Hybrid materials with knitted textile as a support material and aligned high-surface-area nanofibers could represent ideal materials for use in the filtration, optical, and biomedical industries.

KEYWORDS: electrospinning • fiber alignment • nanocomposite • PLLA

One-dimensional and quasi-one-dimensional materials, such as nanofibers, represent a commercially viable class of nanostructures. Their application in a variety of technologies is due to their high surface area and interconnected porous structure. Various techniques for the manufacture and organization of these nanostructures have been developed (1). Electrospinning remains at the forefront for nanofiber production because of its unique combination of versatility, scalability, control of the fiber morphology, and ease with which the encapsulation of active molecules can be achieved (1−5). The versatility of electrospinning allows one to use a wide variety of natural or synthetic polymers for the construct, as well as control over the resultant morphology of the nanofibers. Numerous applications of electrospun fibers have been developed, including those in filtration, biomedical, composite, and electronic and photonic structures (1, 6). Nanofiber formation using electrospinning involves the ejection of a thin jet of material, which is caused by the electrostatic force produced between the charged polymer solution/melt and a metal counter electrode. A stable jet or "Taylor cone" can be produced when the electric field applied is in the range of 15−30 kV. As the electrospinning jet travels to the collector, it is constantly subjected to a stretching movement, leaving behind polymeric nanofibers on the collector as a nonwoven textile.

In general, the collected nanofibers often show random orientation due to the bending and whipping movement of the electrospinning jet. Control over the unidirectional organization of the nanofibers is required to design high-performance, nanofiber-based membranes. Uniaxially oriented fibers are desired for the design of advanced nanofiber-reinforced composites (7). Nanofibers with aligned structures have also been proven to be superior for tissue engineering applications, promoting controlled cell growth, adhesion, and proliferation resembling those of the natural extracellular matrix (8−11). In filtration membranes, oriented fiber structures are expected to produce lower-pressure drops and filtration efficiencies can also be tailored. Aligned fibers are also promising candidates for the design of directional optical components, such as waveguides and lasers based on nanofibers. This has resulted in a growing interest in obtaining anisotropically oriented nanofibers. Several approaches have been developed to obtain aligned electrospun fibers, with most of these techniques relying upon either the patterning of electrodes using a dual-grounded collection plate (12) and parallel auxiliary electrodes (13) and/or the modification of the fiber collection system using a rotating tube collector (14) or a copper wire collector (15). The parallel electrode method has received more attention because of the higher degree of alignment that can be achieved (16).

Another problem persists for the commercial viability of nanofiber membranes: ultrathin electrospun membranes generally lack structural integrity. This problem can be addressed by using blended systems, by post-treatment, and by using composites materials (17). Hierarchically organized nanofiber composites have great potential to solve this problem because they allow for interfacing nanofibers with other structural surfaces, and therefore the advantages of both components can be utilized synergistically (18). A commercial success of such a composite is the use of knitted textiles overlaid with electrospun fibers in the filtration industry (19). The nanofiber layer offers high filtration efficiency, and the knitted textile provides structural integrity. These composite materials, with a thin layer of nanofibers on top of the knitted textile, have also been successfully utilized for tissue engineering applications. The superior structural integrity and mechanical strength of the knitted

* Corresponding author. Tel: 860-486-4619. Fax: 860-486-4745. E-mail: sotzing@mail.ims.uconn.edu.
Received for review June 2, 2009 and accepted September 9, 2009
[†] The Polymer Program, Institute of Materials Science, University of Connecticut.
[‡] Teleflex Medical.
[§] Department of Chemistry, University of Connecticut.
DOI: 10.1021/am900382f

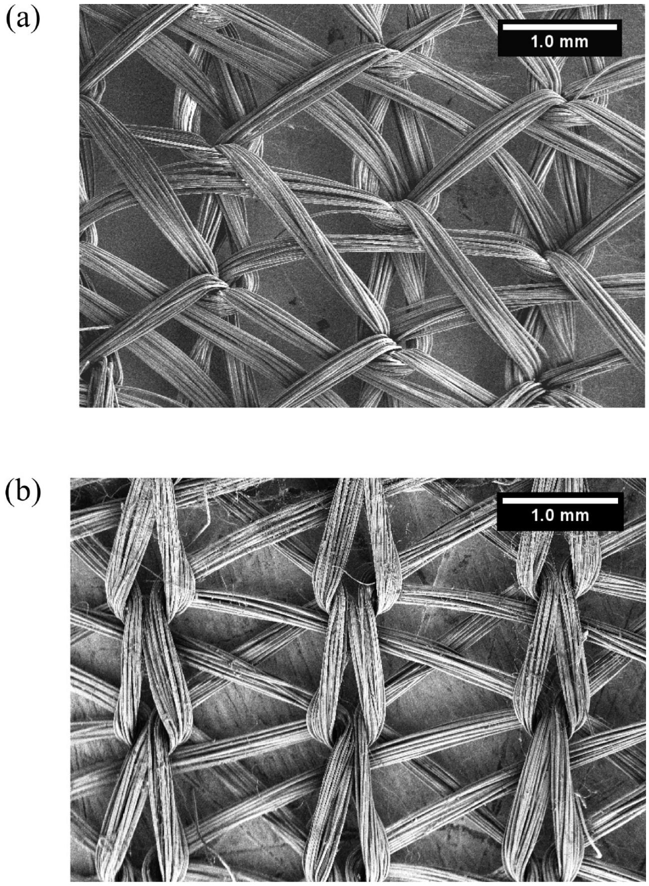

FIGURE 1. SEM images of the PLLA knitted mesh: (a) front side; (b) back side.

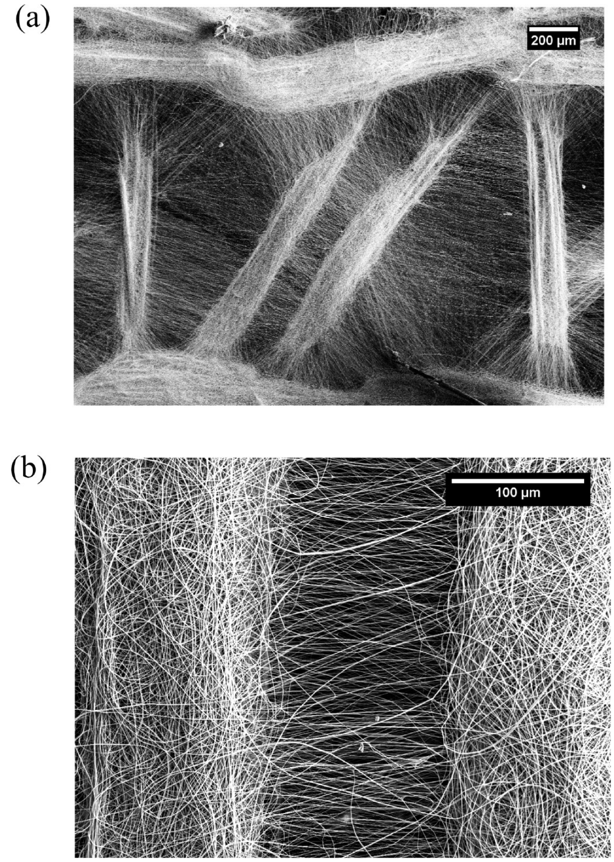

FIGURE 2. SEM images of the PLA nanofiber overlaid on the gold-coated PLLA knitted mesh at different magnifications: (a) 55×; (b) 300×.

microfibers, along with the large surface area and better hydrophilic property of the nanofibers, have been highlighted (20). On the basis of this concept, three-dimensional hybrid materials with alternating layers of micrometer-sized fibers and electrospun nanofibers have been fabricated (17).

The full potential of electrospun nanofibers can only be utilized when they are assembled in well-ordered structures with the desired mechanical stability and structural integrity. The objective of the present study is to describe the formation of well-aligned nanofibers on top of a flexible surface. To the best of our knowledge, no other study has been conducted that indicates the formation of nanofiber composites with oriented nanofibers on top of a flexible structural component. In particular, we communicate the use of a simple technique to pattern oriented poly(lactic acid) (PLA) nanofibers on a poly-L-lactic acid (PLLA) microfiber mesh using a conductive coating. Our approach is to use the knit pattern of the fabric mesh as a conductive electrode and the separation between these patterns as the insulating gap. The conducting layer, gold, is deposited by sputter coating, wherein the knit patterns of the mesh serve as the first point of contact for the parallel electrodes. This configuration results in well-aligned electrospun fibers overlaid atop a flexible knitted fabric.

It has been demonstrated that when a dual-grounded collection electrode is used for fiber alignment, the geometric shape of the conductor and the nature of the insulating gap affect the orientation of the deposited fibers (16, 21, 22). Figure 1 shows a field-emission scanning electron microscopy (FESEM) image of the uncoated PLLA knitted textile from both the front and back of the fabric. The knitted flexible mesh is a multifilament textile mesh designed for soft tissue reinforcement (23−25). For the present study, we have used the back side of the mesh for alignment because each knit pattern line formed from the looping of the yarn serves the purpose of individual conductive electrodes for nanofiber alignment.

The PLLA mesh used in the present study is flexible and therefore needed a solid substrate for support during fabrication. As we observed and as reported by Xia et al. (3, 12), the parallel metal electrodes deposited on a glass slide do not produce any aligned fibers. This is due to the insulating nature of the glass substrate. However, when we deposited parallel gold electrodes on strips of masking tape on the glass substrate, electrospinning resulted in well-aligned fibers (images not shown). The protrusion created by the masking tape was adequate to increase the resistivity of the substrate and resulted in aligned fibers. This result clearly indicates that having a conductively coated mesh affixed to a glass substrate as a support could produce aligned fibers.

Initial experiments were carried out by sputter-coating gold on top of the entire mesh. In all experiments, relatively large area meshes are used (ca. 2.5 cm × 5.0 cm). The sputter-coating time was maintained constant at 25 min. The

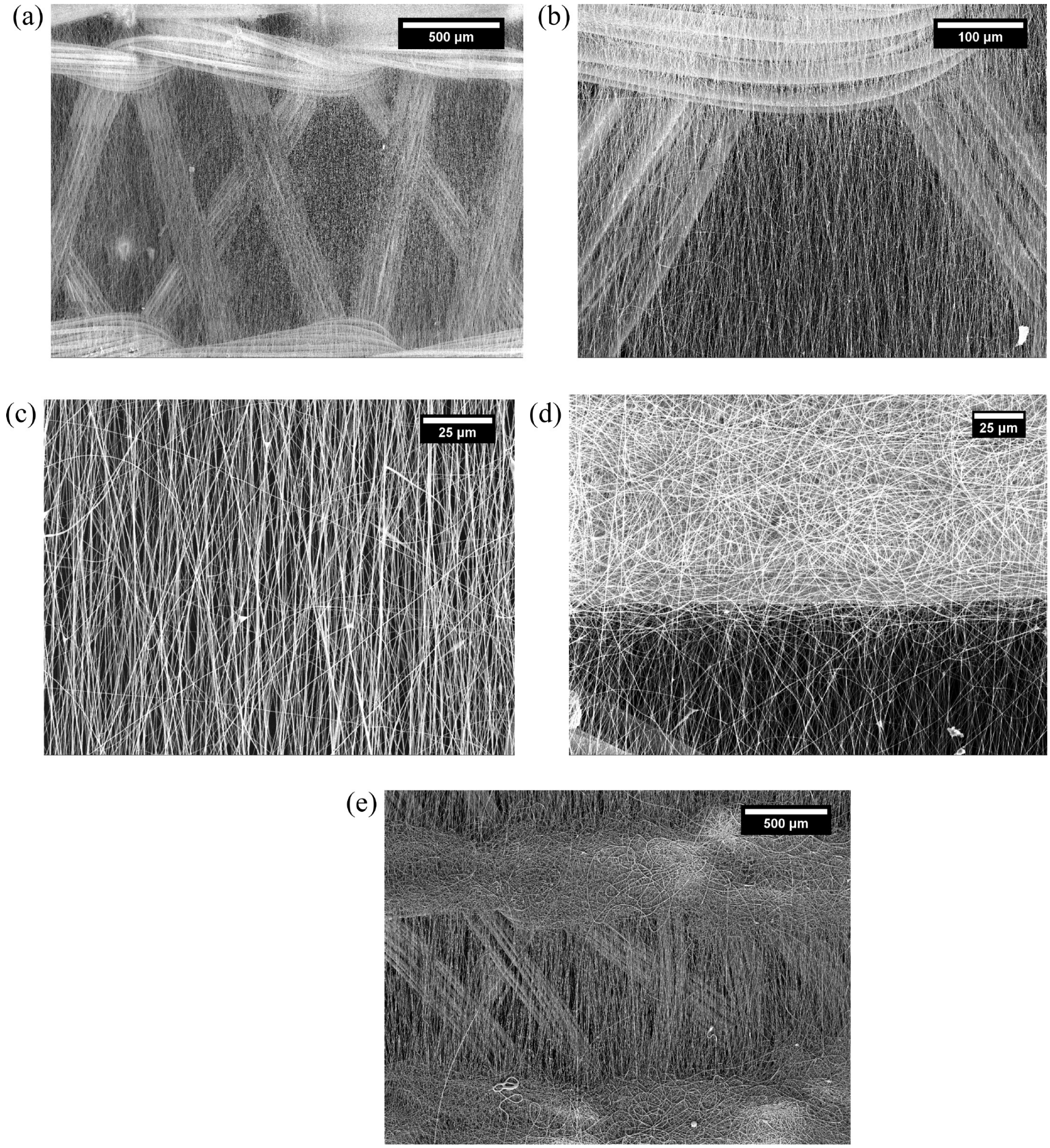

FIGURE 3. SEM images showing the alignment of PLA nanofibers across gold-coated microfiber ridges of a PLLA knitted mesh at various magnifications: (a) 50×; (b) 220×; (c) 500×. (d) Deposition of fibers on gold-coated ridges. (e) Alignment of the thick PLA nanofibers across gold-coated ridges.

surface resistivity of these fabrics was measured to be between 2 and 10 kΩ/cm. Parts a and b of Figure 2 show FESEM images of the resultant PLA nanofibers coated on a knitted PLLA mesh. It was observed that the major alignment occurred between the yarns within the interstitial gaps of the knitted mesh. Interestingly, the ridges created by the knit patterns had no significant involvement in the nanofiber alignment. This result can possibly be attributed to the comparatively large separation (∼1.65 mm) between ridges.

In an effort to obtain aligned fibers between the knit pattern lines (ridges on the mesh), we selectively coated these ridges using the masking tape technique. These gold-patterned meshes were used as the collector for electrospinning. The electrospinning of PLA using an 8.2% (w/w) solution resulted in a thin coating of nanofibers, with an average fiber diameter of 310 nm, on top of the knitted mesh. The FESEM images of the resultant composites are shown in Figure 3a–c. It was concluded that fiber alignment occurred between these gold-coated ridges. These results are significant with respect to manipulating the alignment in the specific direction required on any nonconductive flexible substrates. The mechanism of fiber alignment, using two strips of parallel conductive electrodes, involves drawing of the charged nanofibers onto the electrode closer to them because of stronger electrostatic attraction. During continuous nanofiber drawing, the whipping action due to bending instability causes different sections of the fiber to be preferentially attracted to the closest electrode and results in

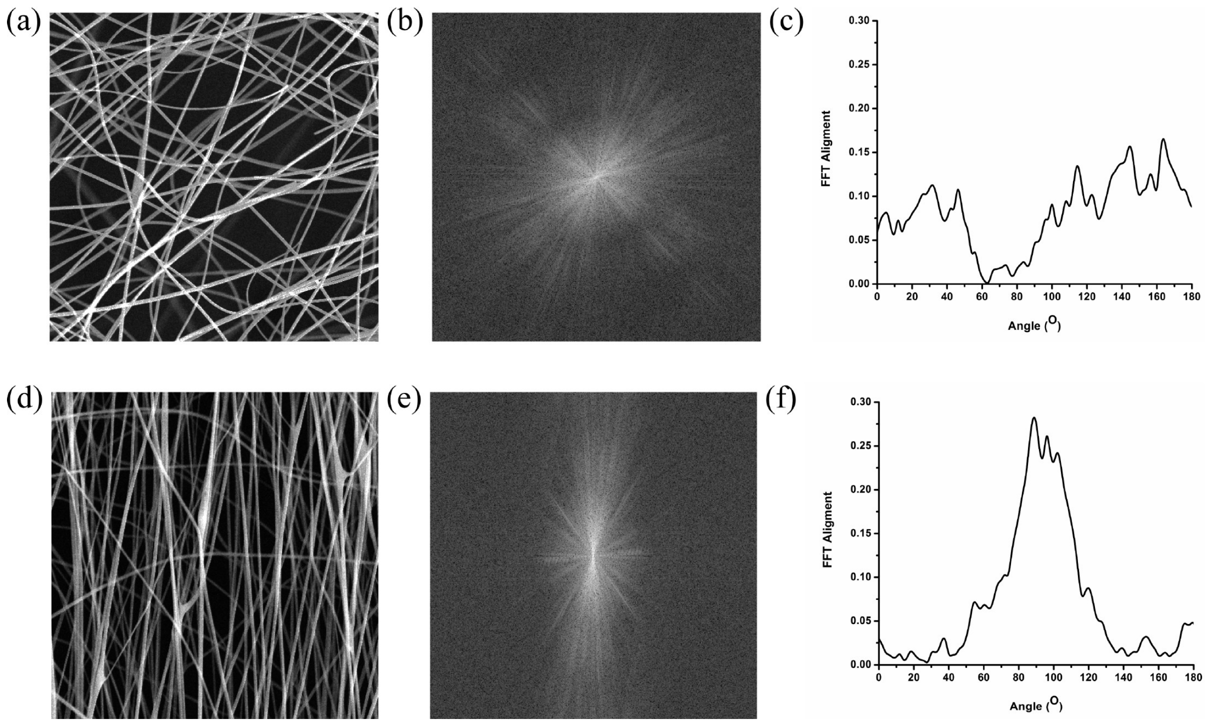

FIGURE 4. SEM images of electrospun fibers obtained on PLLA knitted meshes: (a) without gold coating; (b) FFT output images of part a; (c) pixel intensity plotted against the acquisition angle of part b. SEM images of electrospun fibers obtained on PLLA knitted meshes: (d) with gold coating; (e) FFT output images of part d; (f) pixel intensity plotted against the acquisition angle of part e (FESEM image 32 μm $\times$ 32 μm).

fiber alignment. We conductively coated the ridges on PLLA knitted fabric such that these ridges serve as parallel conductors. As can be seen in Figure 3, metal-coated flexible parallel electrodes behave similarly to those in the parallel metal electrode technique reported by Xia et al. (3, 12). Figure 3d shows the origination of the aligned nanofibers as a result of attraction of the fibers between parallel electrodes. For a further demonstration of the versatility of our approach, we deposited thick electrospun nanofibers with an average diameter of 1.39 μm by spinning from a 15% (w/w) PLA spin dope. This also resulted in the alignment of the fibers between the ridges, as shown in Figure 3e. Liu and Dzenis carried out a detailed investigation of the effects of the electrode gap width, fiber residual charge, and fiber "looping" on the alignment. They concluded that these parameters significantly influence the degree of nanofiber alignment (16). The gap width employed here (1.65 mm) is smaller than that in their study (3 cm); nonetheless, we were able to obtain predominantly uniaxially aligned nanofibers. We hypothesize that this is possible because of the dissipation of residual charge from the nanofibers, as a result of the close proximity of the multiple electrode assemblies (see Figure 2a,b).

Nanofiber alignment is quantified by performing a two-dimensional fast Fourier transform (FFT) analysis on the FESEM images. FFT can be used to convert the geometric characteristics of a spatial domain into a frequency domain. The FFT image contains vital information regarding the frequency distribution in the original image, which can be assessed by the radial summation of pixel intensities in each degree of a circular profile (26). Figure 4 compares the alignments obtained with and without a conductive coating using FFT analysis. In the case of nanofibers electrospun on an uncoated PLLA surgical mesh, only randomly deposited fibers were obtained (Figure 4a). The frequency domain conversion of Figure 4a resulted in a circular symmetrical profile (Figure 4b) indicative of a random distribution of pixel intensities in the original image. On the other hand, the FFT image of aligned fibers obtained using a coated PLLA mesh as a substrate (Figure 4e) resulted in an elliptical profile representing a directional distribution of pixel intensities in the original image. The radial summation of FFT images of unaligned (Figure 4a) and aligned (Figure 4d) nanofibers and subsequent normalization resulted in the two-dimensional FFT alignment plots in parts c and f of Figure 4, respectively. The more intense and narrow peak near 90° in Figure 4f indicates a nearly perfect alignment of nanofibers in a parallel vertical direction. The maximum FFT alignment value for these nanofibers was calculated to be 0.28 at an 89° acquisition angle and percentage ratio FFT alignment values around 90 $\pm$ 30° found to be 78%. These results further illustrate that conductively coated flexible substrates can be used to obtain high-quality aligned nanofibers.

In summary, we have reported a simple technique to obtain aligned fibers atop knitted textile structures. The presented approach of obtaining aligned fibers on a flexible substrate offers several advantages, including the structural benefits from the nanofibers and micromesh, with the collector itself being the structural composite, and the fact that several parallel electrodes can be laid down simultaneously in different geometrical arrangements (similar to electroconductive metal meshes used for alignment) (27), which allows for a greater level of complexity. There is a growing interest in the scientific community for obtaining aligned electrospun fibers because several commercially viable applications require control of the fiber orientation, and results from the present study will strengthen such efforts. In a broader perspective, an extension of this work is likely to lead to the development of composite materials consisting of aligned fibers loaded with therapeutic agents and a gold coating for use in *in vivo* molecular imaging. These results, along with the versatility of electrospinning with respect to control of the fiber diameter, could lead to composite materials of broader applicability.

EXPERIMENTAL SECTION

Materials. Multifilament 75 denier PLLA knitted textile with microfibers of 21.5 μm average diameter was donated by Teleflex Medical (Coventry, CT) and used as received. Electrospinning was carried out using PLA pellets (Natureworks, LLC, Minnetonka, MN) with a M_n = 65 000 g/mol and M_w = 121 000 g/mol (as determined by gel permeation chromatography using polystyrene standards).

Collector Patterning. Sputter coating was carried with a gold target using a Hummer VII (Anatech Ltd., Alexandria, KY) sputter coater. The deposition was carried out at a rate of 4 nm/min (80 mTorr) for 25 min onto the knitted textile placed on the glass slides. Patterned gold lines were deposited in a similar way, except that masking tape was used. After deposition, the masking tape was removed to obtain selective gold coating on the knit patterns.

Electrospinning. A total of 8.2% by weight of a PLA (pellets) solution in 85:15 (w/w) chloroform/*N*,*N*-dimethylformamide was electrospun using the setup described in our previous studies (28, 29). The flow rate was controlled by a KD Scientific programmable infusion pump at 0.18 mL/h. The vertical distance from the spinneret (25 gauge blunt needle) to the collector was maintained at 15 cm. The potential difference of 15 kV was applied between the spinneret and the ground collector. The ambient temperature recorded was 23 °C. A gold-patterned fabric was used as the collector by directly establishing contact between the gold lines and ground wires from the same source.

Microscopy. FESEM images were obtained at various magnifications using a JEOL 6335 field-emission scanning electron microscope to elucidate fiber diameters and their topology across the surface. The samples were coated with gold for 2 min before analysis. The fiber diameter is measured on 50 randomly selected fibers.

FFT Analysis. FFT analysis was performed using *ImageJ* image analysis software (National Institutes of Health). FESEM images with 1500× magnification were cropped to a 512 × 512 pixel area and converted to an 8-bit-type image. Because of the inherent rotation produced in this type of analysis, the FFT image was rotated by 90°. These modified FFT images were then radically summed using an oval profile plug-in between intensities from 0 to 360°. The obtained gray-scale values were normalized as per method described in the literature (26). Because of the repetitive nature of the profile, only the results from 0 to 180° are presented.

Acknowledgment. The authors acknowledge financial support from the CT SBIR Nanotechnology Fellowship Bridge Program. The authors greatly appreciate the donation of materials and technical support from Teleflex Medical.

LETTER

REFERENCES AND NOTES

(1) Huang, Z. M.; Zhang, Y. Z.; Kotaki, M.; Ramakrishna, S. *Compos. Sci. Technol.* **2003**, *63*, 2223–2253.
(2) Bognitzki, M.; Czado, W.; Frese, T.; Schaper, A.; Hellwig, M.; Steinhart, M.; Greiner, A.; Wendorff, J. H. *Adv. Mater.* **2001**, *13*, 70–72.
(3) Li, D.; Wang, Y.; Xia, Y. *Adv. Mater.* **2004**, *16*, 361–366.
(4) Li, W. J.; Laurencin, C. T.; Caterson, E. J.; Tuan, R. S.; Ko, F. K. *J. Biomed. Mater. Res.* **2002**, *60*, 613–621.
(5) Ner, Y.; Grote, J. G.; Stuart, J. A.; Sotzing, G. A. *Angew. Chem., Int. Ed.* **2009**, *48*, 5134–5138.
(6) Chronakis, I. S. *J. Mater. Process. Technol.* **2005**, *167*, 283–293.
(7) Tang, C.; Liu, H. *Composites, Part A* **2008**, *39*, 1638–1643.
(8) Xu, C. Y.; Inai, R.; Kotaki, M.; Ramakrishna, S. *Biomaterials* **2004**, *25*, 877–886.
(9) Lee, C. H.; Shin, H. J.; Cho, I. H.; Kang, Y. M.; Kim, I. A.; Park, K. D.; Shin, J. W. *Biomaterials* **2005**, *26*, 1261–1270.
(10) Baker, B. M.; Mauck, R. L. *Biomaterials* **2007**, *28*, 1967–1977.
(11) Chew, S. Y.; Mi, R.; Hoke, A.; Leong, K. W. *Biomaterials* **2008**, *29*, 653–661.
(12) Li, D.; Ouyang, G.; McCann, J. T.; Xia, Y. *Nano Lett.* **2005**, *5*, 913–916.
(13) Wu, Y.; Carnell, L. A.; Clark, R. L. *Polymer* **2007**, *48*, 5653–5661.
(14) Teo, W. E.; Kotaki, M.; Mo, X. M.; Ramakrishna, S. *Nanotechnology* **2005**, *16*, 918–924.
(15) Katta, P.; Alessandro, M.; Ramsier, R. D.; Chase, G. G. *Nano Lett.* **2004**, *4*, 2215–2218.
(16) Liu, L.; Dzenis, Y. A. *Nanotechnology* **2008**, *19*, 355307.
(17) Kim, G.; Son, J.; Park, S.; Kim, W. *Macromol. Rapid Commun.* **2008**, *29*, 1577–1581.
(18) Teo, W. E.; Ramakrishna, S. *Compos. Sci. Technol.* **2009**, *69*, 1804–1817.
(19) Barhate, R. S.; Ramakrishna, S. *J. Membr. Sci.* **2007**, *296*, 1–8.
(20) Sahoo, S.; Ouyang, H.; Goh, J. C. H.; Tay, T. E.; Toh, S. L. *Tissue Eng.* **2006**, *12*, 91–99.
(21) Kim, G.; Kim, W. *Appl. Phys. Lett.* **2006**, *88*, 233101.
(22) Jalili, R.; Morshed, M.; Ravandi, S. A. H. *J. Appl. Polym. Sci.* **2006**, *101*, 4350–4357.
(23) Lee, J.; Cuddihy, M. J.; Kotov, N. A. *Tissue Eng., Part B* **2008**, *14*, 61–86.
(24) de Tayrac, R.; Chentouf, S.; Garreau, H.; Braud, C.; Guiraud, I.; Boudeville, P.; Vert, M. *J. Biomed. Mater. Res., Part B* **2008**, *85*, 529–536.
(25) Klinge, U.; Schumpelick, V.; Klosterhalfen, B. *Biomaterials* **2001**, *22*, 1415–1424.
(26) Ayres, C. E.; Jha, B. S.; Meredith, H.; Bowman, J. R.; Bowlin, G. L.; Henderson, S. C.; Simpson, D. G. *J. Biomater. Sci., Polym. Ed.* **2008**, *19*, 603–621.
(27) Zhang, D.; Chang, J. *Adv. Mater.* **2007**, *19*, 3662–3667.
(28) Ner, Y.; Grote, J. G.; Stuart, J. A.; Sotzing, G. A. *Soft Matter* **2008**, *4*, 1448–1453.
(29) Jang, S. Y.; Seshadri, V.; Khil, M. S.; Kumar, A.; Marquez, M.; Mather, P. T.; Sotzing, G. A. *Adv. Mater.* **2005**, *17*, 2177–2180.

AM900382F